Journal of Applied Polymer Science

Preparation and characterization of poly(vinyl alcohol) and 1,2,3-propanetriol diglycidyl ether incorporated soy protein isolate-based films

Fengjuan Xu,[1,2,3]* Wei Zhang,[1,2,3]* Shifeng Zhang,[1,2,3] Li Li,[1,2,3] Jianzhang Li,[1,2,3] Yang Zhang[1,2,3]

[1]Key Laboratory of Wooden Material Science and Application (Ministry of Education), College of Materials Science and Technology, Beijing Forestry University, Beijing, China 100083

[2]Beijing Key Laboratory of Wood Science and Engineering, College of Materials Science and Technology, Beijing Forestry University, Beijing 100083, China

[3]Engineering Research Center of Forestry Biomass Materials and Bioenergy (Ministry of Education), College of Materials Science and Technology, Beijing Forestry University, Beijing 100083, China

*The first two authors contributed to this work equally.

Correspondence to: S. Zhang (E-mail: zhangshifeng2013@126.com), L. Li (E-mail: lili630425@sina.com), and J. Li (E-mail: lijianzhang126@126.com)

ABSTRACT: Novel biodegradable films were prepared from soy protein isolate (SPI), poly(vinyl alcohol) (PVA), glycerol, and 1,2,3-propanetriol diglycidyl ether (PTGE). The mechanical, hydrophilic, and compatible properties of the films were investigated. The influence of PTGE as a crosslinker on the properties of the SPI/PVA/PTGE films was examined with Fourier transform infrared spectroscopy, X-ray diffraction (XRD), thermogravimetric analysis, mechanical analysis, contact angle measurements, and scanning electron microscopy. XRD and contact angle examination confirmed that the addition of PTGE altered the film microstructure to a crystalline one. The mechanical properties and water resistance of the SPI/PVA/PTGE films increased notably compared with those of the unmodified SPI films. All results indicate that the networks were formed between SPI and PTGE and played an important role in forming a homogeneous structure in the obtained films. The novel biodegradable films provide a convenient and promising way for preparing environmentally friendly film materials. © 2015 Wiley Periodicals, Inc. J. Appl. Polym. Sci. **2015**, *132*, 42578.

KEYWORDS: biomaterials; crosslinking; films; mechanical properties; proteins

Received 17 July 2014; accepted 4 June 2015

DOI: 10.1002/app.42578

INTRODUCTION

Because they are not sustainable or renewable resources, the use of petroleum-based polymers and composites has caused considerable environmental problems. Interest has recently arisen in the development of fully sustainable and environmentally friendly materials.[1] Among biopolymers, animal and vegetable proteins are practical for making food-packaging films because of their relatively low cost and high availability as byproducts of food processing.[2–5]

With the advantages of renewability, biocompatibility, biodegradability, processability, and film-forming capacity, soy protein isolate (SPI) is a type of protein that has great potential to be used in the food industry, agriculture, bioscience, and biotechnology.[6–8] Particularly, SPI is an interesting alternative for the production of environmentally friendly materials. As an abundant and renewable resource with high biodegradability, these proteins have aroused further interest by researchers.[9,10] However, two major drawbacks in the application of SPI films are their fragility in the wet state and the poor properties of their moisture barrier.[11] Hence, physical, chemical, and enzymatic modifications can be used to improve the functional properties of SPI; these include changing drying conditions and processing method,[12,13] enzymatic treatment with horseradish peroxidase,[14] ultrasound treatment,[15–17] heat curing,[18] ultraviolet irradiation,[19] and blending with hydrophobic additives, such as neutral lipids, fatty acids, waxes, or poly(vinyl alcohol) (PVA).[20,21]

As a nontoxic and synthesized water-soluble polymer with high film-forming, emulsifying, adhesive, and biodegradable abilities,[22,23] PVA is widely used for the preparation of blends and composites with several natural renewable polymers.[24,25] A promising achievement of PVA-modified SPI films has been developed.[26] SPI/PVA films are hydrophilic because the main

Table I. Compositions of the SPI-Based Films

	Content					
Sample	SPI (g)	Glycerol (g)	Water (g)	PVA (g)[a]	PTGE (g)	DMP-30 (g)
A	5	2.5	95	—	—	—
B	5	2.5	95	2.5	—	—
C	5	2.5	95	5	—	—
D	5	2.5	95	7.5	—	—
E	5	2.5	95	5	0.5	—
F	5	2.5	95	5	0.5	0.05

[a] A 10 wt % PVA solution was prepared via the dissolution of pure PVA in water.

chains of SPI and PVA contain abundant hydroxyl groups. Thus, an improvement in the water resistance of the SPI/PVA films is desired to expand their application to the food and nonfood industries.[27]

In this study, 1,2,3-propanetriol diglycidyl ether (PTGE) was used as a crosslinker to improve the mechanical properties and water resistance of the soy-protein-based films and 2,4,6-tris(dimethyl aminomethyl) phenol (DMP-30) was used to catalyze the reaction between the epoxy groups with amino groups.[28,29] A serial of SPI-based films was characterized by X-ray diffraction (XRD) and Fourier transform infrared (FTIR) spectroscopy to illustrate the reaction between SPI and PTGE. The tensile strength (TS), water resistance, and cross-sectional morphology of the resulting films were also investigated.

EXPERIMENTAL

Materials

SPI with 2.0% moisture and 88–95.0% protein was provided by Yuwang Ecological Food Industry Co., Ltd. (Shandong, China). The deionized water, PVA, and glycerol (1,2,3-propane triol, 99.0% purity) and other chemical reactants of analytical grade were purchased from Beijing Chemical Reagents Co., Ltd. (Beijing, China).

Preparation of the SPI Films

The SPI solution was prepared as follows: SPI was added to the deionized water, mixed in a beaker under magnetic stirring, and adjusted to a pH value of 9.0 for 30 min. Then, the modifiers were added to the SPI solution and stirred persistently for 5 min. We removed air bubbles in the previous film-forming solutions by dropping the tributyl phosphate. Finally, the film-forming solution (50 mL) was cast onto Teflon-coated plates and dried at 45°C for 20 h. The SPI-based films were peeled off from plates and remained at room temperature for 48 h before the examination. The composition parts of the films are presented as in Table I.

Mechanical Properties

The mechanical properties of the obtained films (70 × 15 mm^2) were measured by an electronic universal testing machine at a loading speed of 10.0 mm/min (DWD-3020, Changchun Kexin Instrument Co., Ltd., China). We calculated the TS values of the films by dividing the peak loads by the

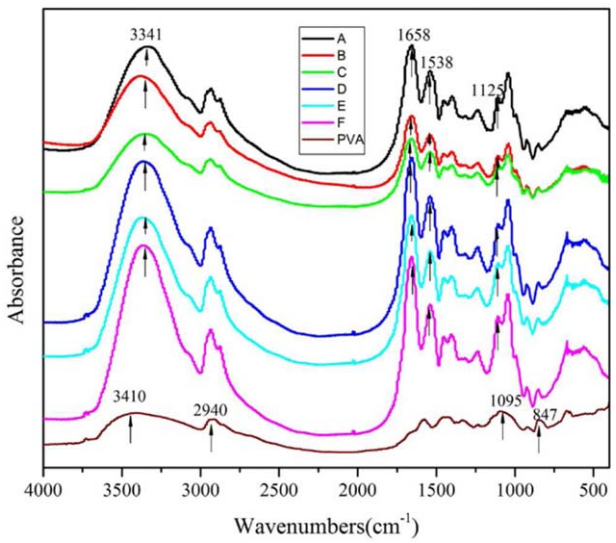

Figure 1. FTIR spectra of the PVA film and SPI-based films. [Color figure can be viewed in the online issue, which is available at wileyonlinelibrary.com.]

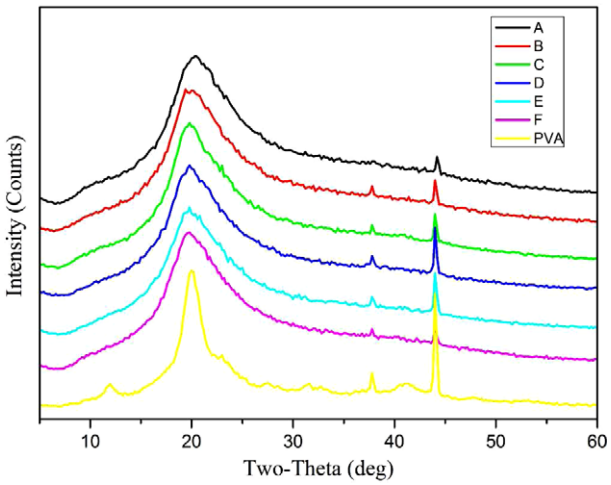

Figure 2. XRD patterns of the PVA film and SPI-based films. [Color figure can be viewed in the online issue, which is available at wileyonlinelibrary.com.]

Table II. Crystallinity of the Blended Films with Different Compositions

Sample	A	B	C	D	E	F	PVA
Relative crystallinity index (%)	24.06	25.27	26.67	27.65	25.04	25.95	36.32
Standard deviation	0.41	0.29	0.47	0.49	0.62	0.58	0.40

The values are presented as the means and standard deviations.

cross-sectional areas of the films.[30] Five replicates were completed for each composition.

Water Uptake

The initial mass (m_i) was determined with an analytical balance ($\pm$0.0001 g). The square-shaped samples (4 cm^2) were immersed in a covered bottle with 50 mL of water at 25°C for 24 h. The water in the bottle was stirred every 6 h before the examination. Then, the water was removed, and the final weight (m_f) was determined. The water uptake was calculated as follows:

$$\text{Water uptake } (\%) = \left(m_f - m_i\right) \times m_i^{-1} \times 100 \quad (1)$$

Five replicates were performed for each composition.[13]

Surface Contact Angle

The surface contact angles of films were measured with an OCA20 contact angle meter (Dataphysics Co., Ltd., Germany). A film sample (20 × 80 mm^2) was placed on a movable carrier and leveled horizontally. A 3-μL drop of distilled water was dropped on the film surface with a microsyringe. The contact angles were measured in a conditioning room. Five replicates were conducted for each film.[31]

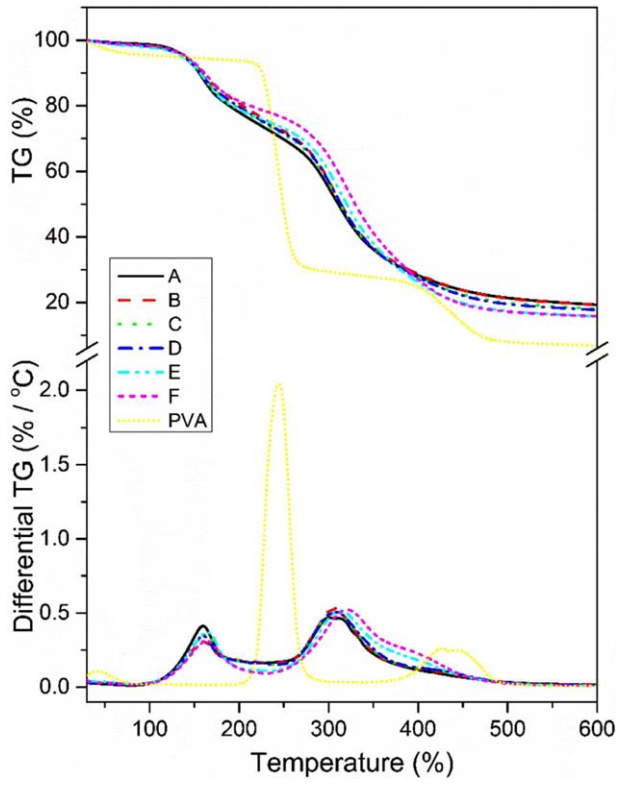

Figure 3. TG and differential TG patterns of the individual PVA and SPI-based films. [Color figure can be viewed in the online issue, which is available at wileyonlinelibrary.com.]

XRD

XRD was performed with an XRD-6000 XRD meter (Shimadzu, Kyoto, Japan) in the continuous scanning mode. The samples were scanned from 5 to 60° (2θ) at 2°/min with the application of Cu Kα radiation with a sampling pitch of 0.2°, a tube voltage of 40.0 kV, and a tube current of 30.0 mA. The relative crystallinity index was calculated directly by the measurement instrument with eq. (2):

$$\text{Relative crystallinity index } (\%) = A_c \times \left(A_c + A_a\right)^{-1} \times 100 \quad (2)$$

where A_c is the area of the crystalline region and A_a is the area of the amorphous region. Three replicates were carried out for each composition.

FTIR

FTIR was performed with a spectrometer (7600, Nicolet Instrument Corp., Madison, WI), and each sample was examined through 32 scans with a resolution of 4 cm^{-1}, ranging from 400 to 4000 cm^{-1}. KBr pellets were prepared by the mixture of 1 mg of powder of the SPI-based films with 100 mg of KBr.

Thermogravimetric Analysis (TGA)

Thermal degradation patterns of the unmodified and modified SPI films were examined with a TGA device (Q50, TA Instruments) in a nitrogen atmosphere. The samples were dried in an air-circulating oven at 103 ± 2°C for 24 h until a constant weight was reached. The samples were then placed in a platinum cup and scanned from a room temperature up to 605°C at a heating rate of 10°C/min. The maximum degradation rate was calculated as the mass at the peak temperature divided by the peak temperature.

Table III. TGA Parameters for the Thermal Degradation of the SPI-Based Films

Film	T_{i1} (°C)	T_{max1} (°C)	T_{i2} (°C)	T_{max2} (°C)
A	135.64	159.82	279.56	300.19
B	135.95	160.95	281.54	305.81
C	136.71	162.85	281.25	306.62
D	136.22	163.09	281.35	306.81
E	137.51	164.10	282.29	313.05
F	141.74	164.02	287.66	320.79
PVA	228.24	244.62	401.44	427.03

T_i, initial temperature of degradation; T_{max}, temperature at maximum degradation rate.

Table IV. Mechanical Properties and Water Uptake Capacity of the Macromolecular Films Examined in This Study

	TS (MPa)		EB (%)		*E* (MPa)		Water uptake (%)	
Sample	Average	SD	Average	SD	Average	SD	Average	SD
A	5.24	0.26	110.36	5.50	33.69	3.20	345.90	7.86
B	5.97	0.20	95.30	3.77	51.57	2.70	336.08	7.18
C	7.05	0.24	78.91	2.30	68.47	2.48	311.90	6.53
D	7.42	0.11	72.06	3.35	72.61	2.83	304.40	9.30
E	7.89	0.09	54.58	4.16	85.16	3.21	58.59	5.84
F	8.02	0.49	45.73	2.90	92.76	3.64	47.66	7.07

E, elasticity modulus; EB, elongation at break; SD, standard deviation.

Scanning Electron Microscopy

The cross-sectional morphologies of the unmodified and modified SPI films were characterized by a field emission scanning electron microscope. The interior portions of the cross planes were exposed by cutting with a surgical blade, mounted on conductive adhesives, gold-sputter-coated, and then observed at 5000 magnifications with an accelerating voltage of 5 kV.

RESULTS AND DISCUSSION

Synthesis and Characterization of the SPI-Based Films

The reaction of different components was measured with FTIR spectroscopy. The spectra of the SPI films showed major peaks at 1658, 1538, and 1230 cm^{-1} (Figure 1), which were characteristic of amide I (C═O stretching), amide II (N—H bending), and amide III (C—N and N—H stretching), respectively.[32] The absorption band at 3341 cm^{-1} was attributed to the free and bound —OH groups in SPI, and the peak at 1125 cm^{-1} was due to the P═O groups stretching in tributyl phosphate. The PVA films exhibited several absorption peaks at 3410, 2940, 1095, and 847 cm^{-1}, which were attributed to the resonance of —OH, $—CH_2$, C—O, and C—C, respectively.[33] The peak of P═O in tributyl phosphate was constant at the same ratio of introduction and thus was used as an interior standard peak. The absorption peak intensity at about 1538 cm^{-1} of the SPI-based films decreased with the addition of PTGE and DMP-30. These outcomes suggest that the interaction between the amino and epoxy groups resulted in a decreasing amino group content.

Figure 2 presents the XRD patterns of the films at different compositions. The pure PVA revealed three distinctive diffraction peaks at a 2θ of 12.0, 20.4, and 22.7°; these corresponded to (100), (101), and (200) planes of PVA, respectively.[34] The peak at 44.5° of 2θ was the crystal plane diffraction composite peaks of $(1\bar{1}1)$, (111), $(2\bar{1}0)$, and (210). The main content of SPI was 7S and 11S globulins, and the content of 11S globulins was much higher than that of 7S globulins. Herein, 11S globulins from SPI film A gave a strong characteristic reflection at 2θ of 21.0°.[35] The peak of PVA at $2\theta \approx 12.0°$ disappeared; the peak of SPI films at $2\theta \approx 21.0°$ gradually shifted to several peaks around 20.0 and 21.0° with increasing PVA content (film B, C and D), and the introduction of PTGE and DMP-30 (film F) converged these peaks into one peak. These diffractograms obviously showed that some interaction occurred between the SPI and PTGE molecules. The calculated crystallinity data (Table II) showed that all of the crystallinities of films A, B, C, and D increased significantly because highly crystalline PVA was introduced into the modified SPI films. The crystallinity of films E and F both decreased slightly with the addition of PTGE and DMP-30 compared with film C; this suggested that the molecular chains could not move smoothly after the formation of the crosslinking networks. These changes were consistent with the FTIR results.

The thermal stabilities of the obtained SPI-based films were investigated by thermogravimetry (TG) examination. The weight loss traces and their differential TG curves recorded

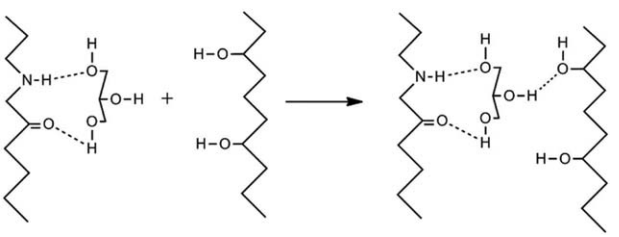

Scheme 1. Formation mechanism of the hydrogen bonds between SPI and PVA.

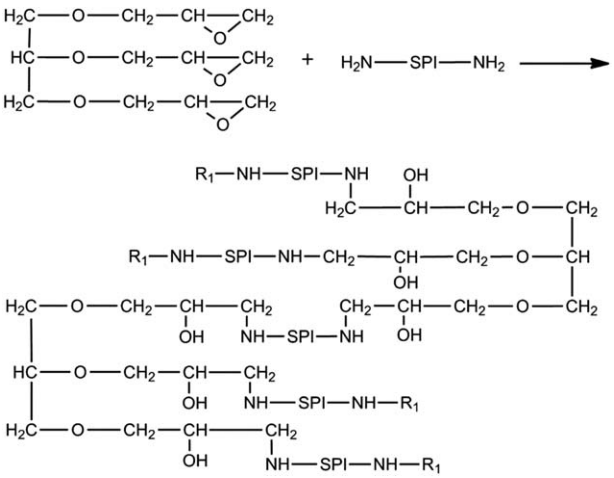

Scheme 2. Reaction mechanism of SPI and PTGE.

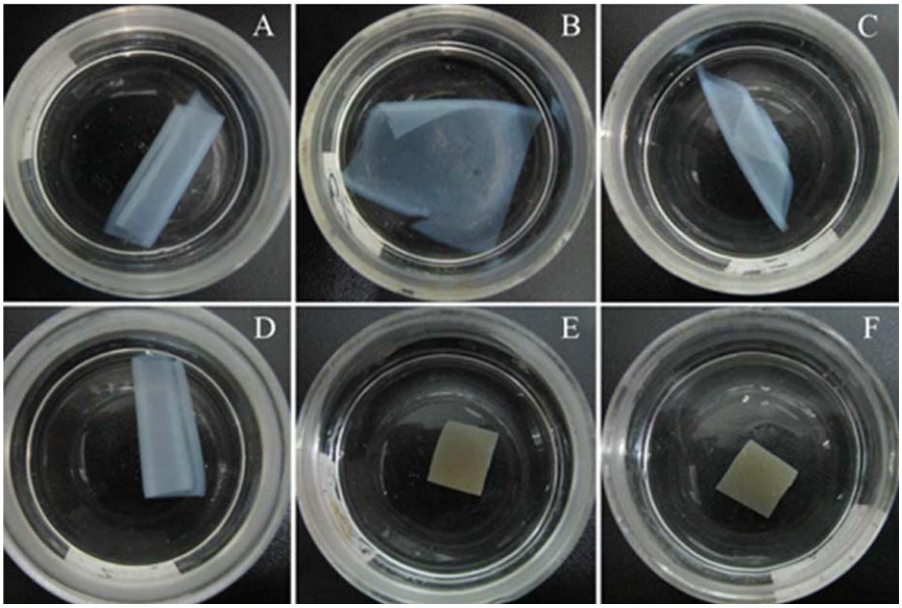

Figure 4. Water uptake of the SPI-based films. [Color figure can be viewed in the online issue, which is available at wileyonlinelibrary.com.]

within 30–600°C are shown in Figure 3. The weight loss within 100–220°C was mainly related to the evaporation of glycerol, and the weight loss from 250 to 450°C was due to the thermal degradation of proteins.[36] As listed in Table III, in the stage of the thermal degradation of proteins, the degradation of PVA began at the initial temperature of 401.44°C and was maximized at 427.03°C. The degradation of the pure SPI film A started at 279.56°C and was maximized at 300.19°C. The initial temperature and the temperature at the maximum degradation rate in the SPI/PVA film D increased to 281.35 and 306.81°C, respectively. Compared to the pure SPI film A, the increases in the temperature were likely due to the presence of the abundant hydrophilic groups that formed interchain hydrogen bonds in the protein chains.[37] The initial temperature and temperature at maximum degradation rate of the SPI/PVA/PTGE films E and F were higher than the decomposition temperatures of the SPI/PVA film C as well. Overall, the enhanced thermal stabilities of the SPI-based films were attributed to the results of the crosslinking reaction between SPI and PTGE.

Mechanical Properties and Water Resistance

The tensile properties define the mechanical response and potential applications of the produced films. Table IV shows the mechanical properties of various SPI-based films. TS was improved from 5.24 to 7.42 MPa after the incorporation of 10% PVA because PVA molecules contained abundant —OH groups and formed strong hydrogen bonds with SPI or intramolecular hydrogen bonds (Scheme 1). Compared to the SPI/PVA film C, PTGE and DMP-30 jointly increased TS from 7.05 to 8.02 MPa; this was probably due to the ring-opening polymerization between epoxy and amino groups (Scheme 2). The PTGE/PVA modified films showed better mechanical properties than the same content of genipin-modified ones; this probably resulted from the higher crosslinking density.[38] With the statistical analysis (analysis of variance), a significant difference

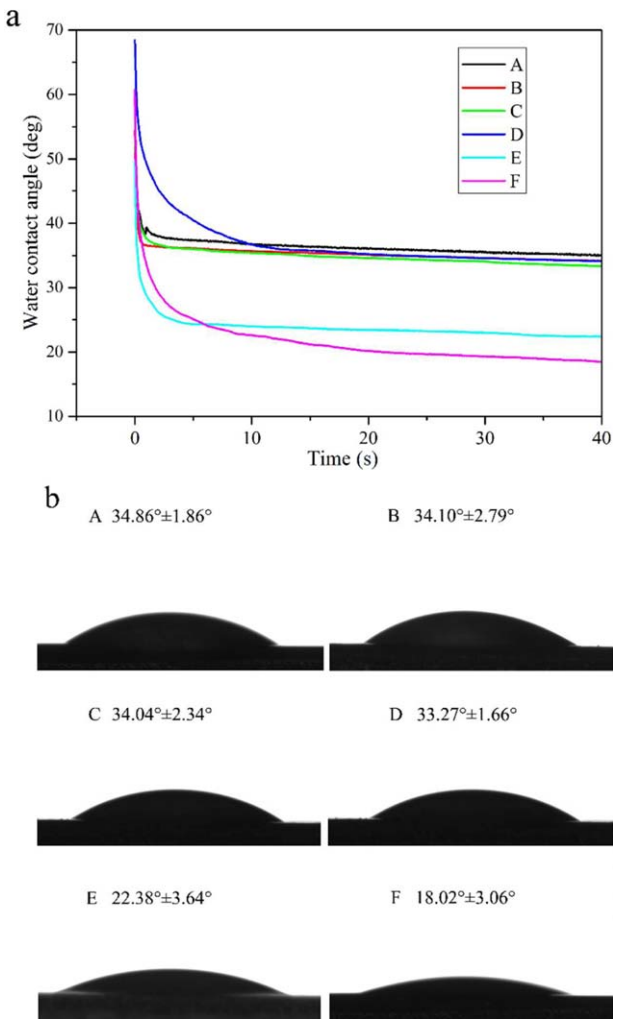

Figure 5. (a) Dynamic WCAs of the SPI-based films and (b) photographs of water droplets on the film surfaces at 20 s. [Color figure can be viewed in the online issue, which is available at wileyonlinelibrary.com.]

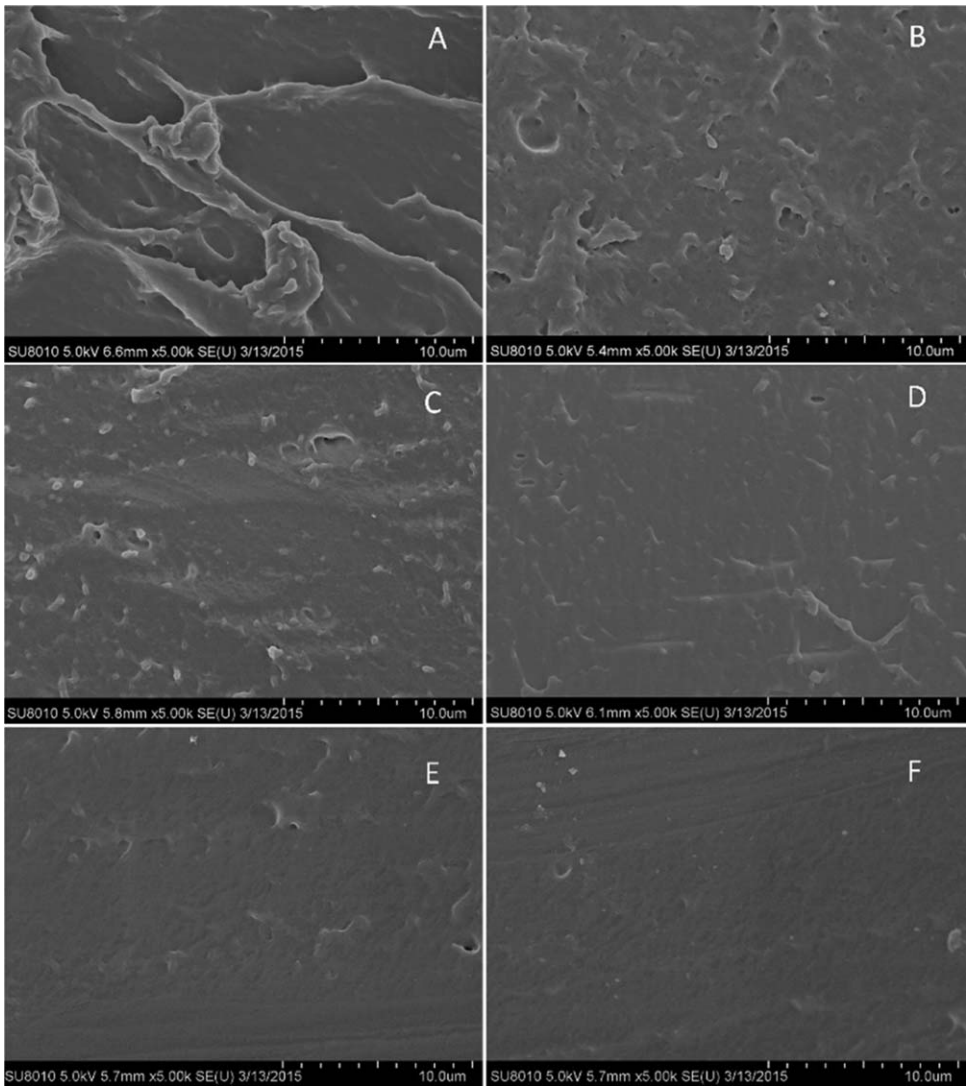

Figure 6. Cross-sectional scanning electron microscopy photographs of the SPI-based films (magnification = 5000×).

($p < 0.01$) was found between samples C and E. Figure 4 presents the morphology of the films after the water absorption. Although the water absorptions of A, B, C, and D was all very high, the water uptake of E and especially F decreased considerably with the incorporation of PTGE and DMP-30. In the gelatin-modified SPI films, when the ratio of SPI/gelatin was 9 : 1, because of the lower crosslinking density, the water uptake of the film was 500%; this was much higher than that of the PTGE/PVA modified film.[39] These results demonstrate that the crosslinked network structure was formed between PTGE and SPI and increased the water resistance of the modified SPI films.

Protein molecules include many chemical bonds, such as hydrogen bonds and amino, carboxyl, and hydroxyl groups. When they were treated with alkaline solution at high temperatures, the internal forces between protein molecules were weakened; this damaged the original network structure between molecules and broke the big stable network structure into smaller ones. This consisted of hydrogen bonds and amino, carboxyl, hydroxyl, and other bonds.[40] As a results, the water uptake of the treated films decreased because the crosslinked network formed in the film. This finding was consistent with the FTIR and XRD results.

Surface Hydrophilicity

The surface hydrophilic properties of the films were investigated by contact angle tests. Figure 5 shows the contact angle as a function of time [Figure 5(a)] and their photos after 20 s [Figure 5(b)]. For all of the films, the water contact angles (WCAs) sharply decreased in the first 10 s but did not decrease significantly after 10 s. As shown in Figure 5, the WCA of the pure SPI film was 34.86°. With increasing content of PVA, the WCA of films decreased from 34.86 to 33.27°, whereas the standard deviations were high; this indicated that no significant change in the WCAs of samples A, B, C, and D was found. It was probably ascribed to the abundant —OH groups forming strong hydrogen bonds with SPI or intramolecular hydrogen bonds of

PVA. The WCAs of films E and F (22.38 and 18.02°) were much lower compared with those of samples A, B, C, and D; this indicated that the surface hydrophilicity of the obtained films increased with the addition of PTGE. The surface chemical composition influenced the wettability of the substance.[41] In waterborne-polyurethane-modified SPI films, when waterborne polyurethane addition was 10%, the contact angle of the film was 45°; this was caused by the incorporation of more hydrophobic polyurethane. The WCA decrease in the PTGE/PVA modified films resulted from more hydrophilic groups formed in the crosslinking reaction.[42] The results are consistent with our previous studies.[43–45]

Film Morphology

Figure 6 shows the cross sections of the SPI-based films. The defects and inhomogeneous characteristics were obvious in the pure SPI film A. The films with the incorporation of PVA (films B, C, and D) resulted in smoother and relatively homogeneous cross sections due to the hydrogen-bond interactions between SPI and PVA. Cross sections of the films modified by PTGE and DMP-30 were more continuous and compact; this was probably due to the crosslinking structural formation in these PTGE-modified films. These results were consistent with the previous tests.

CONCLUSIONS

Because of the formation of the crosslink structure, the PTGE-modified biopolymer films obtained in this study had a higher TS (8.02 MPa) and a higher water resistance (47.66%) compared with the SPI/PVA films. The PTGE-modified SPI biopolymer films exhibited excellent mechanical strength and water resistance because the epoxy groups of PTGE were opened by SPI and formed a chemical crosslinking structure. The findings in this study provide a feasible method for the preparation of crosslinking biopolymer films that could be applied in the packing, biochemical, and chemical industries.

ACKNOWLEDGMENTS

This research was supported by the Special Fund for Forestry Research in the Public Interest (project 201504502), the Beijing Natural Science Foundation (project 2151003), and the National Natural Science Foundation of China (project 31000268/C160302).

REFERENCES

1. Huang, X. S.; Anil, N. *Compos. Sci. Technol.* **2009**, *69*, 1009.
2. Janjarasskul, T.; Krochta, J. M. *Annu. Rev. Food Sci. Technol.* **2010**, *1*, 415.
3. Mangavel, C.; Rossignol, N.; Perronnet, A.; Barbot, J.; Popineau, Y.; Gueguen, J. *Biomacromolecules* **2004**, *5*, 1596.
4. Paetau, I.; Chen, C. Z.; Jane, J. *J. Ind. Eng. Chem.* **1994**, *33*, 1821.
5. Reddy, N.; Yang, Y. *J. Appl. Polym. Sci.* **2013**, *130*, 729.
6. Khan, M. K. I.; Schutyser, M. A. I.; Schroën, K.; Boom, R. *J. Food Eng.* **2012**, *108*, 410.
7. Monedero, F. M.; Fabra, M. J.; Talens, P.; Chiralt, A. *J. Food Eng.* **2009**, *91*, 509.
8. Song, F.; Tang, D. L.; Wang, X. L.; Wang, Y. Z. *Biomacromolecules* **2011**, *12*, 3369.
9. Nishinari, K.; Fang, Y.; Guo, S.; Phillips, G. O. *Food Hydrocolloids* **2014**, *39*, 301.
10. Cui, Z. M.; Kong, X. Z.; Chen, Y. M.; Zhang, C. M.; Hua, Y. F. *Food Hydrocolloids* **2014**, *41*, 1.
11. Andreuccetti, C.; Carvalho, R. A.; Galicia-García, T.; Martínez-Bustos, F.; Grosso, C. R. F. *J. Food Eng.* **2011**, *103*, 129.
12. Denavi, G.; Tapia-Blácido, D. R.; Añón, M. C.; Sobral, P. J. A.; Mauri, A. N.; Menegalli, F. C. *J. Food Eng.* **2009**, *90*, 341.
13. Ciannamea, E. M.; Stefani, P. M.; Ruseckaite, R. A. *Food Hydrocolloids* **2014**, *38*, 193.
14. Stuchell, Y. M.; Krochta, J. M. *J. Food Sci.* **1994**, *59*, 1332.
15. Jambrak, A. R.; Lelas, V.; Mason, T. J.; Krešic, G.; Badanjak, M. *J. Food Eng.* **2009**, *93*, 386.
16. Hu, H.; Wu, J. H.; Chan, E. C. Y. L.; Zhu, L.; Zhang, F.; Xu, X. Y.; Fan, G.; Wang, L. F.; Huang, X. J.; Pan, S. Y. *Food Hydrocolloids* **2013**, *30*, 647.
17. Wang, Z.; Zhou, J.; Wang, X. X.; Zhang, N.; Sun, X. X.; Ma, Z. S. *Food Hydrocolloids* **2014**, *35*, 51.
18. Gennadios, A.; Ghorpade, V. M.; Weller, C. L.; Hanna, M. A. T. *T. Asabe* **1996**, *39*, 575.
19. Gennadios, A.; Rhim, J. W.; Handa, A.; Weller, C. L.; Hanna, M. A. *J. Food Sci.* **1998**, *63*, 225.
20. Rhim, J. W.; Wu, Y.; Weller, C. L.; Schnepf, M. *Sci. Aliment.* **1999**, *19*, 57.
21. Rhim, J. W. *Food Sci. Biotechnol.* **2004**, *13*, 528.
22. Huang, Y. F.; Wu, P. F.; Zhang, M. Q.; Ruan, W. H.; Giannelis, E. P. *Electrochim. Acta* **2014**, *132*, 103.
23. Bonilla, J.; Fortunati, E.; Atarés, L.; Chiralt, A.; Kenny, J. M. *Food Hydrocolloids* **2014**, *35*, 463.
24. Corti, C.; Antone, D. *Prog. Polym. Sci.* **2003**, *28*, 963.
25. Bolto, B.; Tran, T.; Hoang, M.; Xie, Z. L. *Prog. Polym. Sci.* **2009**, *34*, 969.
26. Su, J. F.; Huang, Z.; Yang, C. M.; Yuan, X. Y. *J. Appl. Polym. Sci.* **2008**, *110*, 3706.
27. Wang, S. Y.; Ren, J. L.; Kong, W. Q.; Gao, C. D.; Liu, C. F.; Peng, F.; Sun, R. C. *Cellulose* **2014**, *21*, 495.
28. Liu, X. H.; Wang, J. F.; Yu, J.; Zhang, M. M. *Int. J. Biol. Macromol.* **2013**, *60*, 309.
29. Liu, X. H.; Wang, J. F.; Li, S. H. *Ind. Crops Prod.* **2014**, *52*, 633.
30. Sivarooban, T.; Hettiarachchy, N. S.; Johnson, M. G. *Food Res. Int.* **2008**, *41*, 781.
31. Guerrero, P.; Nurhanani, Z. A.; Kerry, J. P. De la; Caba, K. *J. Food Eng.* **2011**, *107*, 41.
32. Chen, L.; Subirade, M. *Biomacromolecules* **2009**, *10*, 3327.
33. Naveen Kumar, H. M. P.; Prabhakar, M. N.; Venkata Prasad, C.; Madhusudhanrao, K.; Ashok Kumar Reddy, T. V.;

Chowdojirao, K.; Subha, M. C. S. *Carbohydr. Polym.* **2010**, *82*, 251.

34. Assender, H. E.; Windle, A. H. *Polymer* **1998**, *39*, 4295.
35. Chen, J.; Chen, X. Y.; Zhu, Q. J.; Chen, F. L.; Zhao, X. Y.; Ao, Q. *J. Sci. Food Agric.* **2013**, *93*, 1687.
36. Kumar, R.; Wang, L. X.; Zhang, L. N. *J. Appl. Polym. Sci.* **2008**, *111*, 970.
37. Wu, Q. X.; Zhang, L. N. *Ind. Eng. Chem. Res.* **2001**, *40*, 1879.
38. González, A.; Strumia, M. C.; Alvarez Igarzabal, C. I. *J. Food Eng.* **2011**, *106*, 331.
39. Cao, N.; Fu, Y. *J. Food Hydrocolloids* **2007**, *21*, 1153.
40. Mo, W. M.; Zeng, X. Q.; Zhang, X. Q. *J. Food Sci. Technol. Mys.* **2001**, *22*, 22.
41. Zhang, X.; Li, Z.; Liu, K.; Jiang, L. *Adv. Funct. Mater.* **2013**, *23*, 2881.
42. Tian, H.; Wang, Y.; Zhang, L.; Quan, C.; Zhang, X. *Ind. Crops Prod.* **2010**, *32*, 13.
43. Xu, F. J.; Dong, Y. M.; Zhang, W.; Zhang, S. F.; Li, L.; Li, J. Z. *Ind. Crops Prod.* **2015**, *67*, 373.
44. Li, H. Y.; Li, C. C.; Gao, Q.; Zhang, S. F.; Li, J. Z. *Ind. Crops Prod.* **2014**, *59*, 35.
45. Li, C. C.; Li, H. Y.; Zhang, S. F.; Li, J. Z. *Bioresources* **2014**, *9*, 5448.